

## Synergistic Effect and Drug-Resistance Relief of Paclitaxel and Cisplatin Caused by Co-Delivery Using Polymeric Micelles

Jing Li,<sup>1</sup> Zhihong Li,<sup>2</sup> Minghe Li,<sup>3</sup> Hong Zhang,<sup>2</sup> Zhigang Xie<sup>1</sup>

<sup>1</sup>State Key Laboratory of Polymer Physics and Chemistry, Changchun Institute of Applied Chemistry, Chinese Academy of Sciences, Changchun 130022, People's Republic of China

<sup>2</sup>Department of Thoracic Surgery, The First Hospital of Jilin University, Changchun 130021, People's Republic of China

<sup>3</sup>Department of Oral and Maxillofacial Surgery, School of Stomatology Hospital of Jilin University, Changchun 130021, People's Republic of China

Correspondence to: H. Zhang (E-mail: yveszhang@hotmail.com) and Z. Xie (E-mail: xiez@ciac.ac.cn)

**ABSTRACT:** Combination therapy of paclitaxel (PTX) and cisplatin has been used to treat several cancers in clinic practice, but often causes serious systemic toxicity. Co-delivery of PTX and cisplatin by means of polymeric micelles can reduce the systemic toxicity, but often needs two carrier polymers because of the solubility difference between them. Therefore, a strategy is developed to co-deliver both PTX and cisplatin with only one carrier polymer by encapsulating PTX in the core of a polymeric micelle and cross-linking the micelle with cisplatin. The PTX and Pt contents in the micellar formulation M(PTX/Pt) were 10 and 14 wt %, respectively. *In vitro* cytotoxicity of M(PTX/Pt) was evaluated via 3-(4,5-dimethylthiazol-2-yl)-2,5-diphenyltetrazolium bromide assay in comparison with PTX and its micelle M(PTX), cisplatin and its micelle M(Pt), and PTX/cisplatin combination towards human hepatocarcinoma (SMMC-7721) cells and chemoresistant SMMC-7721(SMMC-7721R) cells. The M(PTX/Pt) exhibited a high synergistic effect in the inhibition of cell growth and proliferation of both SMMC-7721 and SMMC-7721R cells and showed reasonable drug-resistance relief. The synergistic effect and resistance relief were further supported or explained by intracellular uptake measurement of dye-labeled micelles and by the confocal laser scanning microscopy observation of SMMC-7721 and SMMC-7721R cells treated with various formulations. Therefore, M(PTX/Pt) micelles were expected to find potential application in cancer chemotherapy. © 2014 Wiley Periodicals, Inc. *J. Appl. Polym. Sci.* **2015**, *132*, 41440.

**KEYWORDS:** biodegradable; biomedical applications; drug delivery systems

Received 29 June 2014; accepted 25 August 2014

**DOI:** 10.1002/app.41440

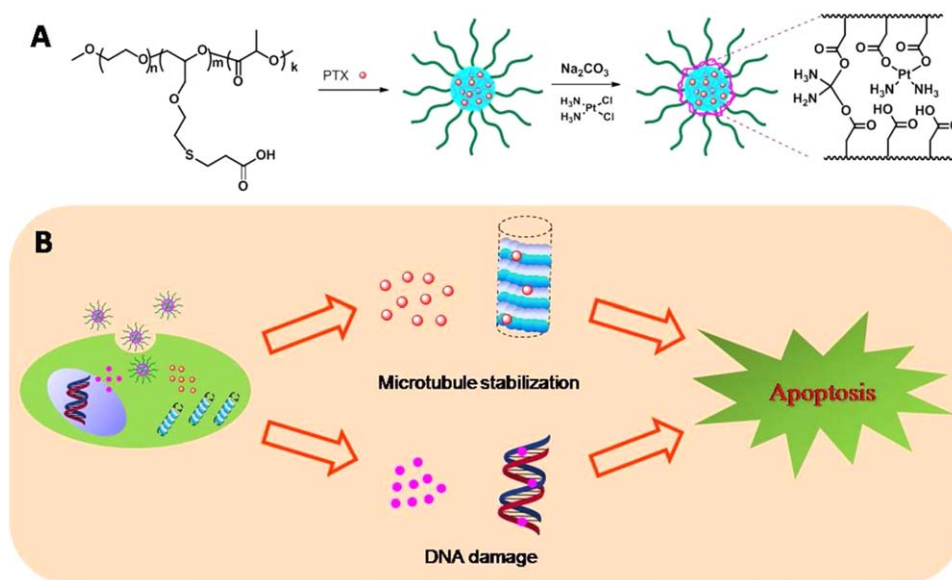
### INTRODUCTION

Cancer metastasis and resistance to chemotherapy is a major hurdle of cancer therapy and result in treatment failure in more than 90% of metastatic cancers. Cancer cells exhibit inherent resistant phenotype because of certain genetic alteration or their acquired resistance following repeated exposure to drugs.<sup>1–5</sup> Although different anticancer therapies could control tumor growth, this control usually is not long lasting. Taking paclitaxel (PTX) as an example, high enough amount of PTX can induce mitotic phase cell death, thereby exerting antitumor effects.<sup>6</sup> PTX-based therapy often improves patient survival; however, the cancer ultimately develops drug resistance in most patients, leading to recurrence of the cancer, distant metastasis and death.<sup>7</sup>

Administering single drug is unlikely to succeed in the treatment of cancer. Therefore, a combination of multiple noncross-resistant anticancer agents has been widely applied clinically.<sup>8–10</sup> Applying multiple drugs with different molecular targets can raise the genetic barriers and delay the cancer adaption process. Multiple drugs targeting the same cellular pathways can function synergistically, giving higher therapeutic efficacy and target selectivity.<sup>11–13</sup> Overall, developing a combined therapeutic approach might even be the key to enhancing anti-cancer efficacy and overcoming chemoresistance.<sup>14</sup> Cisplatin is one of the most widely used DNA-modifying chemotherapy drugs. The combination of PTX/cisplatin free drugs has shown a good synergistic effect against a wide range of cancer cell lines because of the different mechanisms by which PTX and cisplatin act.<sup>15,16</sup>

Additional Supporting Information may be found in the online version of this article.

© 2014 Wiley Periodicals, Inc.



**Scheme 1.** (A) Preparation of M(PTX/Pt). (B) Release of PTX (●) and cisplatin (●) along with microtubule stabilization and DNA damage, resulting in cell apoptosis. [Color figure can be viewed in the online issue, which is available at [wileyonlinelibrary.com](http://wileyonlinelibrary.com).]

Nowadays the combination of PTX/cisplatin free drugs has become the first-line chemotherapy for advanced nonsmall-cell lung cancer,<sup>17</sup> ovarian cancer,<sup>18</sup> advanced gastric cancer,<sup>19,20</sup> advanced breast cancer,<sup>21,22</sup> and metastatic esophageal cancer.<sup>23</sup>

Advances in nanotechnology have opened up unprecedented opportunities for controlled drug delivery and novel combination strategies. In our previous work, the co-delivery of two anticancer drugs using polymeric micelles showed reduced systematic toxicity and greater synergistic effect than combination of two small molecule anticancer drugs both *in vitro* and *in vivo*.<sup>24</sup> Research for other people's work also showed that combination of two antitumor drugs in one nanoparticle could enhance antitumor and antimetastasis efficacy.<sup>25</sup> Actually, nanoparticles are well suited for reversal of the drug resistance because they can ensure delivery of two or more therapeutic agents to the same cell. Wang et al. observed enhanced antitumor efficacy with reduced side effects by co-delivery of doxorubicin and PTX with amphiphilic methoxypoly(ethylene glycol)-b-poly(lactic-co-glycolic acid) (mPEG-PLGA) copolymer nanoparticles.<sup>26</sup> In an attempt to co-encapsulate doxorubicin and cyclosporin A in polyalkylcyanoacrylate nanoparticles, the combined nanoparticle formula showed improved growth inhibition efficacy in a resistant cell culture line.<sup>27</sup> But co-delivery of PTX and cisplatin by co-encapsulation is difficult because cisplatin cannot dissolve easily in either hydrophilic or hydrophobic polymers. By covalent conjugation of PTX and cisplatin, two different carrier polymers are often needed.

In the present study, therefore, polymeric micelles bearing both cisplatin and PTX were constructed by encapsulating PTX in the core of micelles and by incorporating cisplatin into the micelles as a cross-linking agent. Their efficacy towards human hepatocarcinoma (SMMC-7721) cells and PTX-resistant SMMC-7721R cells was examined in comparison with their single use in polymer drug forms or their combination use in small molecular forms.

## MATERIALS AND METHODS

### Materials

PTX was purchased from Chongqing Union Pharmacy, China. Cisplatin was purchased from Shangdong Boyuan Chemical, China. 3,3'-Diocetadecyloxycarbocyanine perchlorate (DiO), 4',6-diamidino-2-phenylindole (DAPI), N-acetyl-L-cysteine (NAC), 3-(4,5-dimethylthiazol-2-yl)-2,5-diphenyltetrazolium bromide (MTT), and dimethyl sulfoxide (DMSO) were purchased from Sigma-Aldrich (St. Louis, MO, USA). (Annexin V-fluorescein isothiocyanate (FITC))/propidium iodide (PI) cell apoptosis kit was obtained from KeyGen Biotech (Nanjing, China). Other chemicals and solvents were obtained commercially and used without further purification.

### Measurements

Transmission electron microscopy (TEM) measurement was performed on a JEOL JEM-1011 transmission electron microscope with an accelerating voltage of 100 kV. Concentrations of cisplatin and PTX were determined by inductively coupled plasma-mass spectrometry (ICP-MS) (Xseries II, ThermoScientific, USA) and high-performance liquid chromatography (HPLC), respectively. The HPLC system consisted of a reverse-phase C-18 column, a mobile phase of acetonitrile and water (65:35 v/v) pumped at a flow rate of 1.0 mL·min<sup>-1</sup> at 25°C. Twenty  $\mu\text{L}$  aliquot of sample was injected, and the column effluent was detected at 227 nm with a UV detector (Waters 2489). PTX concentrations in the samples were determined using a calibration curve of various PTX concentrations (0.1–100  $\mu\text{g}\cdot\text{mL}^{-1}$ ).

### Preparation of PTX Encapsulated Micelles M(PTX)

The poly(ethylene oxide)-block-poly(allyl glycidyl ether)/medroxy progesterone acetate-block-poly-(DL-lactide) (mPEG-b-PAGE-b-PLA), mPEG-b-PAGE/MPA-b-PLA (Scheme 1) was synthesized as previously described.<sup>28</sup> Briefly, 4 mg of PTX and 40 mg of mPEG-b-PAGE/MPA-b-PLA were dissolved in 5 mL

tetrahydrofuran (THF) in a round bottom flask and the solvent was evaporated by rotary evaporation at 40°C to obtain a solid PTX/copolymer film. The obtained thin film was hydrated with 10 mL water at 60°C for 30 min to obtain a micelle solution, which was then filtrated through 0.2 μm filter membrane to remove the unincorporated PTX aggregates, followed by lyophilization to obtain PTX encapsulated micelles M(PTX). The PTX loading content in the micelles was measured by HPLC.

#### Preparation of Cisplatin Complex Micelles M(Pt)

The mPEG-b-PAGE/MPA-b-PLA micelles were prepared using the hydration method according the above description. Cisplatin (0.5 g, 1.67 mmol) was suspended in distilled water and silver nitrate was added ( $\text{AgNO}_3$  : cisplatin = 2 : 1 mol/mol) to form an aqueous complex. The solution was kept in the dark at room temperature for 12 h. The AgCl precipitates formed during the reaction were removed by filtration. The supernatant  $[(\text{NH}_3)_2\text{Pt}(\text{H}_2\text{O})_2(\text{NO}_3)_2]$  was added to the mPEG-b-PAGE/MPA-b-PLA micelle solution and the mixture was stirred for 12 h, followed by dialysis against deionized water with a dialysis bag of cutoff Mw 3500 for 12 h. The micelle solution was freeze-dried. The Pt content in the micelle was measured by ICP-MS.

#### Preparation of PTX/Pt Composite Micelles M(PTX/Pt)

The composite micelles M(PTX/Pt) was prepared similarly to M(Pt) by replacing the blank polymer micelle with PTX-loaded micelle M(PTX) in the previous section.

In order to trace the micelles in the cells, fluorescent dye DiO was employed because of its hydrophobicity similar to PTX and it was encapsulated to PTX-loaded micelles M(PTX) and cisplatin/PTX-loaded micelles M(PTX/Pt) by co-assembly with PTX. The products obtained were coded as M(PTX+DiO) and M(PTX+DiO/Pt), respectively. The content of DiO in the micelles was calculated by measuring its fluorescence standard curves in DMF.

#### Drug Release from the Micelles of M(Pt), M(PTX), or M(PTX/Pt)

Twenty mg of M(Pt), M(PTX), or M(PTX/Pt) was dissolved in 10 mL of phosphate buffer solution (PBS, 0.01 M, containing 0.1% Tween 80). The solution was then placed into a pre-swollen dialysis bag (molecular weight cutoff of 3.5 kDa) and immersed in 40 mL of PBS. The dialysis was conducted at 37°C in a shaking culture incubator. One milliliter of sample was withdrawn from the incubation medium at specified time intervals. After sampling, equal volume of fresh PBS was immediately added into the incubation medium. Platinum and PTX released from the micelles were measured by ICP-MS and HPLC, respectively, and expressed as cumulative percentage of the drug outside the dialysis bag with respect to the total drug in the original micelles.

#### Cell Culture

Human hepatocellular carcinoma cell line SMMC-7721 was provided by the cell bank of the Shanghai Institutes for Biological Sciences. Drug-resistant cell line was established by the stepwise selection with increasing concentration of PTX from 0.005 to 2 μg·mL<sup>-1</sup>. Both cell lines were grown at 37°C in a humidified

atmosphere containing 5% (v/v) CO<sub>2</sub> in dulbecco's minimum essential medium (DMEM) supplemented with 10% fetal bovine serum, and 100 U/mL penicillin and 100 mg/mL streptomycin.

#### In Vitro MTT Assay

Cells harvested in a logarithmic growth phase were seeded in 96-well plates at a density of  $1 \times 10^6$  cells/well and incubated in DMEM for 24 h. The medium was then replaced with various drug formulations of cisplatin, PTX, M(Pt), M(PTX), free PTX/Pt combination, and M(PTX/Pt). All of the drugs with platinum were modulated at a final equivalent Pt concentration from 0.8 to 25 μg·mL<sup>-1</sup>, final equivalent PTX concentration from 0.63 to 20 μg·mL<sup>-1</sup>. The incubation was continued for 48 and 72 h. Then, 20 μL of MTT solution in PBS with the concentration of 5 mg/mL was added and the plates were incubated for another 4 h at 37°C, followed by removal of the culture medium containing MTT and addition of 150 μL of DMSO to each well to dissolve the formazan crystals formed. Finally, the plates were shaken for 10 minutes, and the absorbance of formazan product was measured at 570 nm by a microplate reader.

#### Intracellular Uptake via Confocal Laser Scanning Spectroscopy (CLSM)

About  $1 \times 10^6$  cells/well were seeded in 6-well plates and grown for 24 h prior to incubation with 0.1 mg/mL DiO-loaded micelles M(PTX+DiO) or M(PTX+DiO/Pt). Cells were imaged at 2 h post-treatment using a CLSM. DAPI were used to stain the nuclei. For detecting apoptosis,  $1 \times 10^6$  cells/well were seeded in 6-well plates and grown for 24 h prior to incubation with a final equivalent Pt concentration of 50 μg·mL<sup>-1</sup> and a final equivalent PTX concentration of 40 μg·mL<sup>-1</sup>. The incubation was continued for 2 h. After staining with 5 μL Annexin V-FITC and 10 μL PI (5 μg·mL<sup>-1</sup>) in 1×binding buffer for 15 min at room temperature in the dark and washing with PBS for three times, the cells were visualized with CLSM (TCS SP5, Leica, Germany).

#### Statistical Analysis

Data were expressed as means ± standard deviation (SD) from at least three experiments. Statistical analyses were carried out using a statistics program (GraphPad Prism; GraphPad Software). One-way ANOVA was used to compare the treatment effects.  $P < 0.05$  was considered to be statistically significant.

## RESULTS AND DISCUSSION

#### Synthesis and Characterization of Polymer-Drug Micelles

The synthesis and characterization of mPEG-b-PAGE/MPA-b-PLA copolymer and its <sup>1</sup>H NMR spectrum and the assignments of protons were detailed in our previous paper.<sup>28</sup> The mPEG-b-PAGE/MPA-b-PLA copolymer was self-assembled to form core-shell-corona micelles. The three domains provided different functions: the hydrophobic PLA inner core was for PTX or PTX+DiO entrapment, the PAGE/MPA middle shell with carboxyl groups for cisplatin chelation and micelle cross-linking, and the PEG corona for protection and water solubility. To achieve co-loading of PTX and cisplatin, a two-step procedure was adopted: Initially, PTX was loaded into the inner core by hydration of copolymer thin films. After that, conjugation of

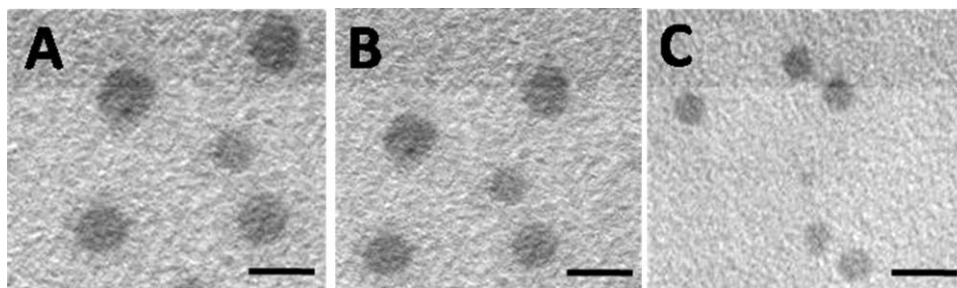


**Figure 1.** TEM images of (A) M(PtX), (B) M(Pt), and (C) M(PtX/Pt) (scale bar = 50 nm).

cisplatin to the middle PAGE/MPA shell was carried out in aqueous medium for 12 h. Three kinds of micelles were prepared: M(PtX) and M(Pt) contained PTX or cisplatin alone, while M(PtX/Pt) contained both of them at the weight ratio of PTX/Pt = 0.7 as determined by ICP-MS and HPLC.

As shown in Figure 1, the mean diameters of M(Pt) (1A), M(PtX) [Figure 1(B)] and M(PtX/Pt) [Figure 1(c)] micelles were 41, 42, and 17 nm, respectively. M(PtX/Pt) was smaller than the other two. The cross-linking was beneficial for stable drug delivery during blood circulation. The size distribution widths of the micelles are near or less than 50 nm, which makes them qualified as drug delivery systems.

#### Drug Release from the Micelles

To evaluate the release behavior of the dual-drug-loaded micelles, we carried out the cisplatin and PTX release at 37°C in buffered solution (pH 7.4, containing 0.1% Tween 80). The release of cisplatin from the nanoparticles was because of the ligand exchange reaction of cisplatin from the carboxylates to the chloride ions in physiological saline. As shown in Figure 2, PTX showed a faster release rate from M(PtX) than cisplatin from M(Pt) under the same condition, which can be attributed to the physical entrapment of PTX compared to the ligand chelation of cisplatin. However, the release rate of the entrapped PTX was evidently retarded in M(PtX/Pt) because of the middle shell cross-linking caused by platinum chelation. In 72 h, 58.5% PTX was released from M(PtX), while only 39.9% was released from M(PtX/Pt) at the same time. It is noticed that Pt release from M(PtX/Pt) was slower than that from M(Pt), probably because of possible interference of hydrophobic PTX toward Pt complex hydrolysis.

#### Cytotoxicity of Micelles

Cisplatin is classified as alkylating agent; its cytotoxicity is thought to result from inhibition of DNA synthesis in cancer cells.<sup>29,30</sup> PTX is a microtubule stabilizing drug and a potent chemotherapeutic agent that has shown substantial clinical efficacy for various solid tumors.<sup>31–35</sup> Furthermore, it has been shown *in vitro* that the cytotoxicity of PTX is more dependent on the exposure time than on increased PTX concentration.<sup>36–40</sup> Although the combination chemotherapy of paclitaxel and cisplatin using polymer prodrug strategy could lead to enhanced antitumor efficacy, the mechanism of apoptosis was not clear.<sup>24</sup> The *in vitro* cytotoxicity of the micelles was evaluated by using MTT assay. Firstly, the cell compatibility of the blank micelles was examined. As shown in Figure 3, cell viability of both

SMMC-7721 cells (PTX-sensitive) and SMMC-7721R cells (PTX-resistant) cells was maintained above 86% and 82%, respectively, at all tested concentrations after 48 and 72 h incubation. Therefore, the micelle carrier materials in the form of micelles were not toxic and well tolerated by the tested cells. Next, the proliferation inhibition effects of PTX, cisplatin, PTX/Pt, M(Pt), M(PtX) and M(PtX/Pt) on SMMC-7721 and SMMC-7721R cells were evaluated. Results were collected in Figure 4. First of all, cell inhibition of each formulation exhibited both dose and time dependence. Based on the dose dependence,  $IC_{50}$  (concentration for 50% inhibition) for all formulations were calculated and listed in Table I. Generally,  $IC_{50}$  values at 72 h were lower than the corresponding ones at 48 h. SMMC-7721R cells showed higher  $IC_{50}$  values than the parent SMMC-7721 cells for both PTX and cisplatin and their combination, indicating that SMMC-7721R is both PTX and cisplatin resistant, although it was cultured from SMMC-7721 by feeding PTX only. The ratio of  $IC_{50}$  for SMMC-7721R over  $IC_{50}$  for SMMC-7721, defined as “resistance index (RI)”, of each formulation was calculated and listed in Table I. Because the RI determined at 72 h is comparable to that determined at 48 h, only the  $IC_{50}$  and RI data determined at 48 h will be discussed in the next paragraphs for simplicity.

Firstly, Figure 4 and Table I compare the cytotoxicity of PTX and M(PtX), PTX and M(PtX) displayed almost equal  $IC_{50}$  values towards SMMC-7721 cells ( $3.57 \mu\text{g}\cdot\text{mL}^{-1}$ ) but M(PtX) gave lower  $IC_{50}$  towards SMMC-7721R than PTX

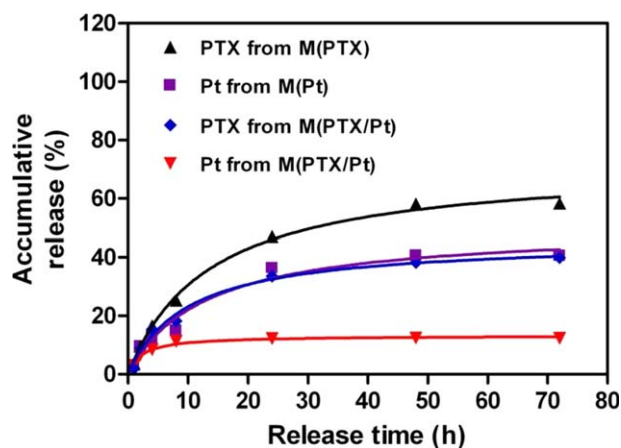


**Figure 2.** Release profiles of M(Pt), M(PtX), M(PtX/Pt) in PBS solution (pH 7.4, containing 0.1% Tween 80) at 37°C. [Color figure can be viewed in the online issue, which is available at [wileyonlinelibrary.com](http://wileyonlinelibrary.com).]



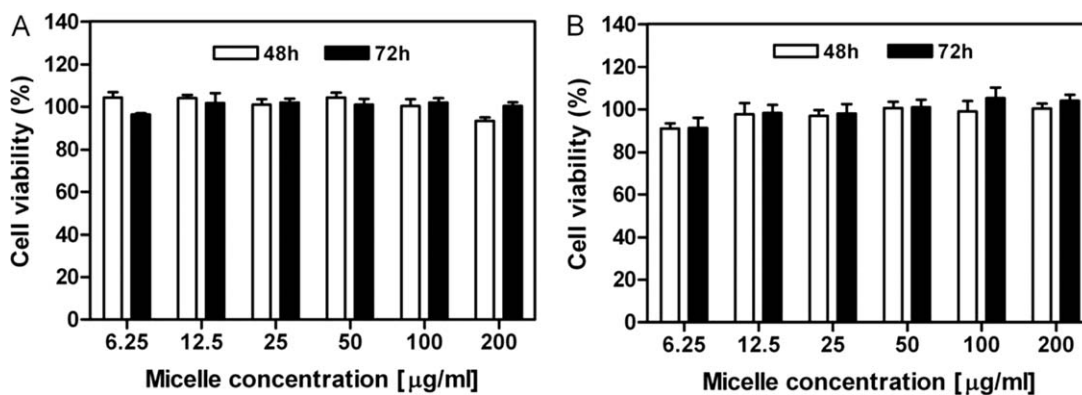


**Figure 3.** *In vitro* cytotoxicity profiles of blank micelles against (A) SMMC-7721 cells and (B) SMMC-7721R cells at 48 and 72 h.

(3.13 vs. 4.17  $\mu\text{g}\cdot\text{mL}^{-1}$ ). Therefore M(PTX) exhibited a lower RI than PTX (0.88 vs. 1.17). It reflected a capability of M(PTX) in relieving drug resistance to some extent compared with PTX itself. While, as shown in Supporting Information Figure S1 and Table I, M(Pt) showed less  $\text{IC}_{50}$  values towards both SMMC-7721 and SMMC-7721R cells than cisplatin, indicating enhanced cytotoxicity of cisplatin after micelle formation. But their RI values were comparable (1.22 vs. 1.29).

Comparing the  $\text{IC}_{50}$  and RI of PTX/Pt combination with those of PTX, cisplatin, and M(PTX/Pt), it was found that: (1) the PTX/cisplatin combination exhibited much less  $\text{IC}_{50}$  values than individual cisplatin and PTX did, indicating a synergistic effect of them towards both SMMC-7721 and SMMC-7721R cells; (2) polymeric combination M(PTX/Pt) showed further less  $\text{IC}_{50}$

values than all other formulations, implying enhanced synergistic effect of PTX and cisplatin in the polymeric micelle form; and (3) PTX/Pt combination exhibited an RI of 1.80 while this value of M(PTX/Pt) was 1.44, showing a mediate drug-resistance relief. In summary, M(PTX/Pt) is the best in inhibiting cancer cell growth and in relieving drug resistance.

#### Intracellular Uptake of M(PTX+DiO) and M(PTX+DiO/Pt)

In order to visualize the drug-loaded micelles taken by the cells, the micelles were labeled with DiO dye and the cells were incubated with DiO-labeled micelles M(PTX+DiO) or M(PTX+DiO/Pt) (DiO content of 0.1  $\text{mg}\cdot\text{mL}^{-1}$ ) for 2 h before CLSM observation. Figure 5 shows the CLSM images of SMMC-7721 or SMMC-7721R cells. Because the cells were thoroughly washed, the fluorescence of DiO (green in the images) is

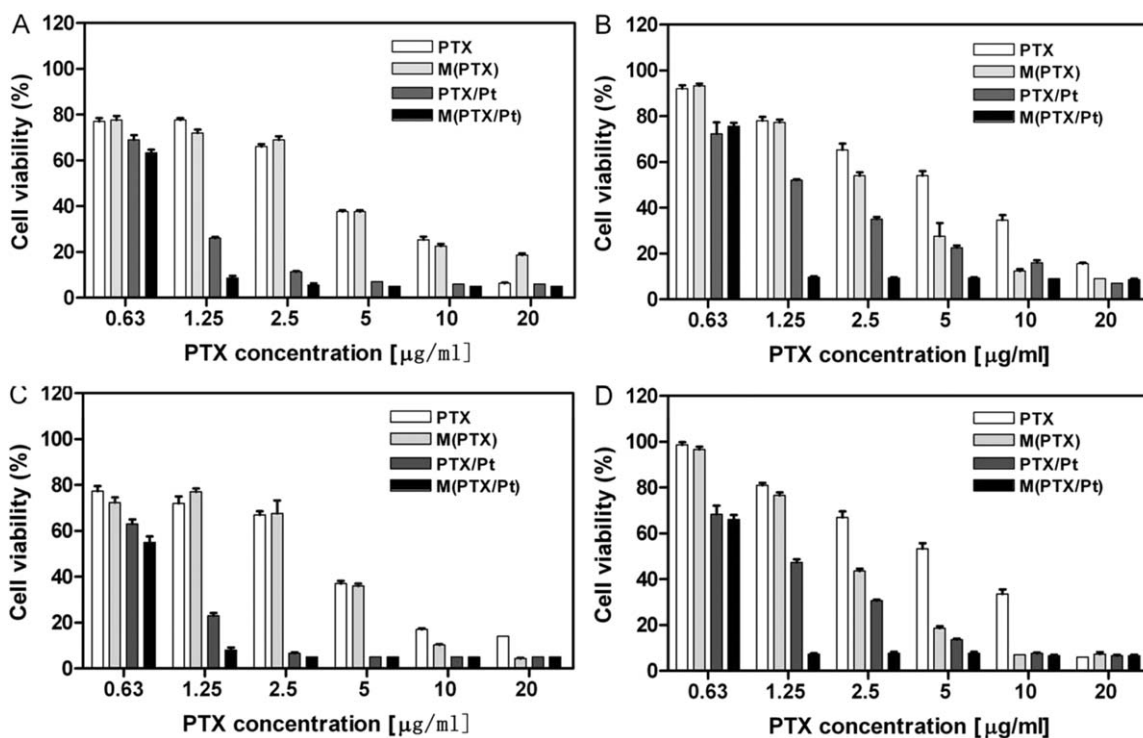


**Figure 4.** *In vitro* cytotoxicity profiles of cisplatin, PTX, PTX/Pt, M(Pt), M(PTX) and M(PTX/Pt) against SMMC-7721 cells (A, C) and SMMC-7721R cells (B, D) at 48 h (A, B) and 72 h (C, D).

**Table I.** IC<sub>50</sub> Values ( $\mu\text{g}\cdot\text{mL}^{-1}$ ) and Resistance Indexes (RI) of Tested Drug Formulations

Formulation	48 h			72 h		
	SMMC-7721	SMMC-7721R	RI	SMMC-7721	SMMC-7721R	RI
PTX	3.57	4.17	1.17	3.56	4.15	1.17
M(PTX)	3.57	3.13	0.88	3.55	2.77	0.78
Cisplatin	1.59	1.94	1.22	1.31	1.89	1.44
M(Pt)	1.38	1.78	1.29	1.38	1.75	1.27
PTX/Pt	1.14/1.43	2.05/2.56	1.80	1.04/1.30	1.83/2.29	1.76
M(PTX/Pt)	0.98	1.37	1.40	0.87	1.25	1.44

believed to come from the micelles taken inside the cells. The cell nucleus was stained with DAPI (blue). At 2 h, the green fluorescence in the cells increased greatly, which suggested that more and more micelles were internalized and the endocytosis velocity of M(PTX+DiO) or M(PTX+DiO/Pt) micelles was quite high. The CLSM images also displayed that the green fluorescence was not only full of the cell plasma, but also came from the nucleus region. It implied that the DiO dye can stain

cell nuclei. Moreover, it was found that use of M(PTX+DiO/Pt) micelles resulted in brighter and size-reduced cell nuclei (B, D) in comparison with the M(PTX+DiO)-treated cells (A, C). It indicates that the platinum species had entered the cell nuclei and caused damages in them, such as nuclear fragmentation and karyopyknosis.

Next, we examined the ability of drug formulations to induce apoptosis in SMMC-7721 and SMMC-7721R cells. Apoptosis or

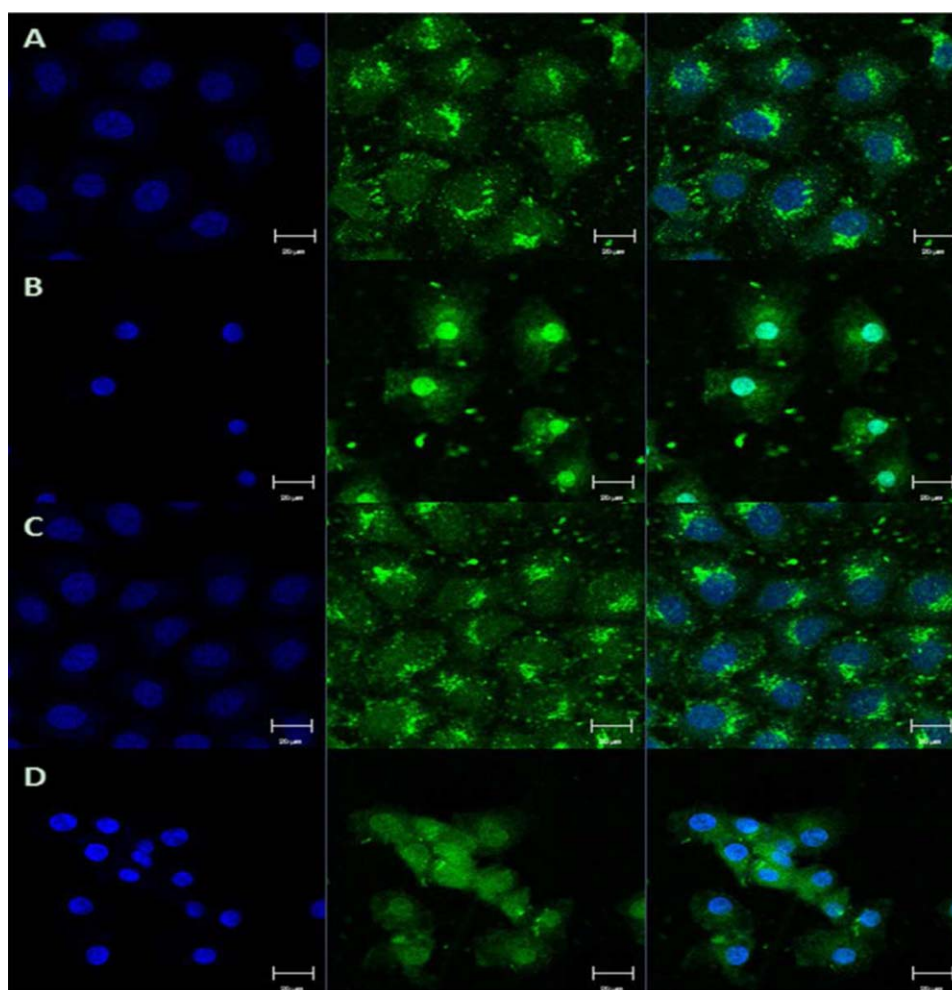


**Figure 5.** CLSM images of SMMC-7721 cells (A and B) and SMMC-7721R cells (C and D) incubated with micelles M(PTX+DiO) (A and C) and micelles M(PTX+DiO/Pt) (B and D) at an equiv. DiO content of  $0.1 \text{ mg}\cdot\text{mL}^{-1}$  for 2 h. Left: DAPI-stained nuclei image; middle: M(PTX+DiO) or M(PTX+DiO/Pt) micelles image; right: merged image. [Color figure can be viewed in the online issue, which is available at [wileyonlinelibrary.com](http://wileyonlinelibrary.com).]

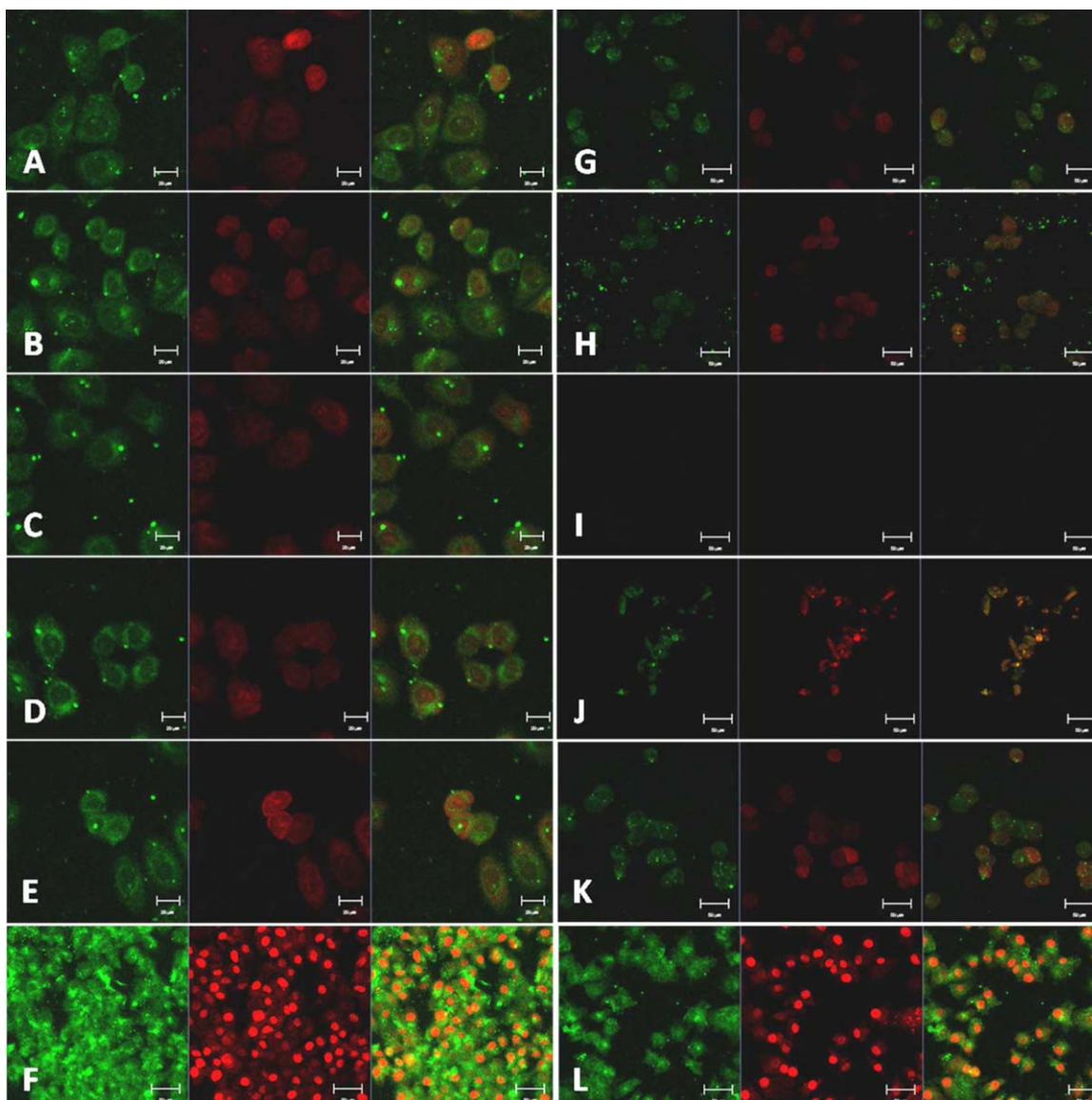


**Figure 6.** CLSM images of SMMC-7721 cells (A–F) and SMMC-7721R cells (G–L) stained with (Annexin V-FITC)/PI after cells were incubated for 2 h with cisplatin (A and G), M(Pt) (B and H), PTX (C and I), M(PTX) (D and J), PTX/Pt (E and K), and M(PTX/Pt) (F and L). Cisplatin conc.:  $50 \mu\text{g}\cdot\text{mL}^{-1}$ ; PTX conc.:  $40 \mu\text{g}\cdot\text{mL}^{-1}$ . Left: (Annexin V)-FITC-stained cell image; middle: PI-stained nuclei image; right: merged image. Scale bars:  $50 \mu\text{m}$ . [Color figure can be viewed in the online issue, which is available at [wileyonlinelibrary.com](http://wileyonlinelibrary.com).]

programmed cell death plays a crucial role in maintaining cellular homeostasis between cell division and cell death.<sup>41,42</sup> Cell death mediated by apoptosis results in a series of morphological changes such as nuclear condensation, nuclear fragmentation, and cell surface blebbing, which leads to the formation of membrane bound vesicles (apoptotic bodies) being subsequently phagocytosed by macrophages.<sup>43</sup> Therefore, the cell death induced by the drug formulations was examined using optical microscope. Cells were incubated with PTX, PTX/Pt or M(PTX/Pt) for 2 h. As shown in Supporting Information Figure S2, M(PTX/Pt) showed significantly more apoptotic morphology in both SMMC-7721 and SMMC-7721R cells compared with other formulations.

Annexin V-FITC together with PI has been widely used as fluorescent probe to distinguish viable cells from dead cells of

different stages.<sup>44,45</sup> Usually green fluorescence from Annexin V-FITC indicates early apoptosis of cells while red fluorescence from PI indicates cell necrosis. In the present study, therefore, the cells treated with various drug formulations for 2 h were labeled with both Annexin V-FITC and PI and then were examined under CLSM. As shown in Figure 6, panels E and L are entirely different from the others in that both green and red fluorescence are very intense and the cell or nuclear size is greatly reduced. In panel J, size reduction is also observed. This is in agreement with Figure 4(B,D) and is ascribed to the damages caused by the platinum species released in the cells. Because the cell treatment is identical, so great difference of M(PTX/Pt)-treated cells implies great potential of this formulation in inducing cell apoptosis. In addition, two tendencies may be found in Figure 6: (1) all right panels (SMMC-7721R cells)



show less cell apoptosis and necrosis than the left panels (SMMC-7721 cells) do, indicating stronger drug resistance of SMMC-7721R cell line than its parent one. (2) One-to-one comparison of panels B, D, and F with panels A, C, and E indicates that micellar formulations M(PTX), M(Pt), and M(PTX/Pt) are a little bit more effective than small molecular ones, respectively. This is also in agreement with the IC<sub>50</sub> data in Table I.

## CONCLUSIONS

In summary, the present study provided a synthetic strategy to use one carrier polymer for one platinum-based drug and one or more other drugs to realize their conjugation, co-assembly, and combination therapy. The synergistic effects were demonstrated *in vitro* for M(PTX/Pt) in both SMMC-7721 and SMMC-7721R cell lines by MTT assay and IC<sub>50</sub> determination, and was further supported and explained by the intracellular uptake measurement of the DiO-labeled micelles and by the CLSM observation of (Annexin V-FITC)/PI dual fluorescence of the drug-treated cells. Although the drug-resistant cell line used is not satisfactory enough (its resistance index is only 1.2–1.8), the micellar formulations, especially M(PTX/Pt) micelles, display improved drug resistance in comparison with the small molecular ones. In short, co-delivery of paclitaxel and cisplatin in a platinum-cross-linked polymeric micellar form not only results in synergistic effect in inhibition of cancer cell growth and proliferation, but also helps relieve drug resistance. Therefore, this strategy is expected to find potential clinic use in cancer chemotherapy, especially for drug resistant patients.

## ACKNOWLEDGMENTS

The project was supported by the National Natural Science Foundation of China (Project No 91227118 and 51373167).

## REFERENCES

1. Cuong, N. V.; Hsieh, M. F.; Chen, Y. T.; Liao, I. *J. Appl. Polym. Sci.* **2010**, *117*, 3694.
2. Zhang, L.; Fu, J. Y.; Xia, Z. X.; Wu, P.; Zhang, X. F. *J. Appl. Polym. Sci.* **2011**, *122*, 758.
3. Varaprasad, K.; Ravindra, S.; Reddy, N. N.; Vimala, K.; Raju, K. M. *J. Appl. Polym. Sci.* **2010**, *116*, 3593.
4. Dai, Z.; Huang, Y.; Sadee, W. *Curr. Top. Med. Chem.* **2004**, *4*, 1347.
5. Gou, P. F.; Liu, W. W.; Mao, W. W.; Tang, J. B.; Shen, Y. Q.; Sui, M. H. *J. Mater. Chem. B* **2013**, *1*, 284.
6. Rodriguez-Antona, C. *Pharmacogenomics* **2010**, *11*, 621.
7. Doyle-Lindrud, S. *Clin. J. Oncol. Nurs.* **2012**, *16*, 286.
8. Boulikas, T.; Vougiouka, M. *Oncol. Rep.* **2004**, *11*, 559.
9. Shoji, T.; Takatori, E.; Omi, H.; Kumagai, S.; Yoshizaki, A.; Yokoyama, Y.; Mizunuma, H.; Fujimoto, T.; Takano, T.; Yaegashi, N.; Tase, T.; Nakahara, K.; Kurachi, H.; Nishiyama, H.; Sugiyama, T. *Int. J. Gynecol. Cancer* **2011**, *21*, 44.
10. Patil, Y.; Sadhukha, T.; Ma, L.; Panyam, J. *J. Control. Release* **2009**, *136*, 21.
11. Lehar, J.; Krueger, A. S.; Avery, W.; Heilbut, A. M.; Johansen, L. M.; Price, E. R.; Rickles, R. J.; Short, G. F., 3rd; Staunton, J. E.; Jin, X.; Lee, M. S.; Zimmermann, G. R.; Borisy, A. A. *Nat. Biotechnol.* **2009**, *27*, 659.
12. Liu, T.; Zhang, Y. F.; Liu, S. Y. *Chinese J. Polym. Sci.* **2013**, *31*, 924.
13. Wang, Y. G.; Yang, T. Y.; Wang, X.; Dai, W. B.; Wang, J. C.; Zhang, X. A.; Li, Z. Q.; Zhang, Q. A. *J. Control. Release* **2011**, *149*, 299.
14. Deng, Z. J.; Morton, S. W.; Ben-Akiva, E.; Dreaden, E. C.; Shopsowitz, K. E.; Hammond, P. T. *ACS Nano* **2013**, *7*, 9571.
15. Huang, G. C.; Liu, S. Y.; Lin, M. H.; Kuo, Y. Y.; Liu, Y. C. *Jpn. J. Clin. Oncol.* **2004**, *34*, 499.
16. Jekunen, A. P.; Christen, R. D.; Shalinsky, D. R.; Howell, S. B. *Br. J. Cancer* **1994**, *69*, 299.
17. Comella, P.; Filippelli, G.; De Cataldis, G.; Massidda, B.; Frasci, G.; Maiorino, L.; Putzu, C.; Mancarella, S.; Palmeri, S.; Cioffi, R.; Roselli, M.; Buzzi, F.; Milia, V.; Gambardella, A.; Natale, D.; Bianco, M.; Ghiani, M.; Masullo, P. *Ann. Oncol.* **2007**, *18*, 324.
18. Levasseur, L. M.; Greco, W. R.; Rustum, Y. M.; Slocum, H. K. *Cancer Chemother. Pharmacol.* **1997**, *40*, 495.
19. Hayashi, T.; Yoshizawa, M.; Watanabe, N.; Murayama, Y.; Shimizu, H. *Gan To Kagaku Ryoho.* **2006**, *33*, 1167.
20. Koneri, K.; Hirono, Y.; Fujimoto, D.; Sawai, K.; Morikawa, M.; Murakami, M.; Goi, T.; Iida, A.; Katayama, K.; Yamaguchi, A. *J. Gastric Cancer* **2013**, *13*, 58.
21. Frasci, G.; Panza, N.; Comella, P.; Nicoletta, G. P.; Natale, M.; Manzione, L.; Bilancia, D.; Cioffi, R.; Maiorino, L.; De Cataldis, G.; Belli, M.; Micillo, E.; Mascia, V.; Massidda, B.; Lorusso, V.; De Lena, M.; Carpagnano, F.; Contu, A.; Pusceddu, G.; Comella, G. *J. Clin. Oncol.* **1999**, *17*, 2316.
22. Frasci, G.; D'Aiuto, G.; Comella, P.; Apicella, A.; Thomas, R.; Capasso, I.; Di Bonito, M.; Carteni, G.; Biglietto, M.; De Lucia, L.; Maiorino, L.; Piccolo, S.; Bianchi, U.; D'Aniello, R.; Lapenta, L.; Comella, G. *Breast Cancer Res. Treat.* **1999**, *56*, 239.
23. Huang, J.; Zhou, Y.; Zhang, H. T.; Qu, T.; Mao, Y. S.; Zhu, H. X.; Quan, L. P.; Xing, P. Y.; Wang, J. W.; He, J.; Xu, N. Z.; Sun, Y. *Med. Oncol.* **2013**, *30*, 343.
24. Xiao, H.; Song, H.; Yang, Q.; Cai, H.; Qi, R.; Yan, L.; Liu, S.; Zheng, Y.; Huang, Y.; Liu, T.; Jing, X. *Biomaterials* **2012**, *33*, 6507.
25. Song, W.; Tang, Z.; Zhang, D.; Zhang, Y.; Yu, H.; Li, M.; Lv, S.; Sun, H.; Deng, M.; Chen, X. *Biomaterials* **2014**, *35*, 3005.
26. Wang, H.; Zhao, Y.; Wu, Y.; Hu, Y. L.; Nan, K. H.; Nie, G. J.; Chen, H. *Biomaterials* **2011**, *32*, 8281.
27. Soma, C. E.; Dubernet, C.; Bentolila, D.; Benita, S.; Couvreur, P. *Biomaterials* **2000**, *21*, 1.
28. Wang, R.; Hu, X. L.; Yue, J.; Zhang, W. J.; Cai, L. Y.; Xie, Z. G.; Huang, Y. B.; Jing, X. B. *J. Mater. Chem. B* **2013**, *1*, 293.
29. Li, Q.; Tian, Y. T.; Li, D. D.; Sun, J. F.; Shi, D. L.; Fang, L.; Gao, Y.; Liu, H. Y. *Biomaterials* **2014**, *35*, 6462.



30. Wang, X.; Yang, C. C.; Zhang, Y. J.; Zhen, X.; Wu, W.; Jiang, X. Q. *Biomaterials* **2014**, *35*, 6439.
31. Lovat, F.; Ishii, H.; Schiappacassi, M.; Fassan, M.; Barbareschi, M.; Galligioni, E.; Gasparini, P.; Baldassarre, G.; Croce, C. M.; Vecchione, A. *Oncotarget* **2014**, *5*, 970.
32. Risinger, A. L.; Riffle, S. M.; Lopus, M.; Jordan, M. A.; Wilson, L.; Mooberry, S. L. *Mol. Cancer* **2014**, *13*, 41.
33. Zhang, D. S.; Yang, R. H.; Wang, S. X.; Dong, Z. *Drug Des. Dev. Ther.* **2014**, *8*, 279.
34. Lee, S.; Lee, Y.; Briggs, J. M.; Lee, K. W. B. *Kor. Chem. Soc.* **2013**, *34*, 1972.
35. Sharma, S.; Lagiseti, C.; Poliks, B.; Coates, R. M.; Kingston, D. G. I.; Bane, S. *Biochemistry* **2013**, *52*, 2328.
36. Tan, D. S. P.; Yap, T. A.; Hutka, M.; Roxburgh, P.; Ang, J.; Banerjee, S.; Grzybowska, E.; Gourley, C.; Gore, M. E.; Kaye, S. B. *Eur. J. Cancer* **2013**, *49*, 1246.
37. Steinfeld, D. S.; Liu, A. P.; Hsu, S. H.; Chan, Y. F.; Stankus, J. J.; Pacetti, S. D.; Tai, J. T. *J. Cardiovasc. Pharmacol.* **2012**, *60*, 179.
38. Das, V.; Miller, J. H. *Eur. J. Neurosci.* **2012**, *35*, 1705.
39. Tokuda, E.; Seino, Y.; Arakawa, A.; Saito, M.; Kasumi, F.; Hayashi, S.; Yamaguchi, Y. *Breast Cancer Res. Treat.* **2012**, *133*, 427.
40. Liebmann, J. E.; Cook, J. A.; Lipschultz, C.; Teague, D.; Fisher, J.; Mitchell, J. B. *Br. J. Cancer* **1993**, *68*, 1104.
41. Ghobrial, I. M.; Witzig, T. E.; Adjei, A. A. *Ca-a Cancer J. Clin.* **2005**, *55*, 178.
42. Kwon, H. J.; Hong, Y. K.; Kim, K. H.; Han, C. H.; Cho, S. H.; Choi, J. S.; Kim, B. W. *J. Ethnopharmacol.* **2006**, *105*, 229.
43. Kroemer, G.; Galluzzi, L.; Vandenabeele, P.; Abrams, J.; Alnemri, E. S.; Baehrecke, E. H.; Blagosklonny, M. V.; El-Deiry, W. S.; Golstein, P.; Green, D. R.; Hengartner, M.; Knight, R. A.; Kumar, S.; Lipton, S. A.; Malorni, W.; Nunez, G.; Peter, M. E.; Tschopp, J.; Yuan, J.; Piacentini, M.; Zhivotovsky, B.; Melino, G. *Cell Death Differ.* **2009**, *16*, 3.
44. Thomas, A. P.; Saneesh Babu, P. S.; Asha Nair, S.; Ramakrishnan, S.; Ramaiah, D.; Chandrashekar, T. K.; Srinivasan, A.; Radhakrishna Pillai, M. *J. Med. Chem.* **2012**, *55*, 5110.
45. Verderio, P.; Bonetti, P.; Colombo, M.; Pandolfi, L.; Prospero, D. *Biomacromolecules* **2013**, *14*, 672.